INITIAL DEVELOPMENT OF A *BLURRY* INJECTOR FOR BIOFUELS

Claudia Gonçalves de Azevedo, claudia@lcp.inpe.br
Fernando de Souza Costa, fernando@lcp.inpe.br
National Institute for Space Research, Associated Laboratory of combustion and Propulsion, Rodovia Presidente Dutra, km 40, Cachoeira Paulista, SP, 12630-000, Brazil

Heraldo da Silva Couto, heraldo.couto@vsesa.com.br
Vale Energy Solution, Rodovia Presidente Dutra, km 138, São José dos Campos, SP, 12247-004, Brazil

Abstract. *The increasing costs of fossil fuels, environmental concerns and stringent regulations on fuel emissions have caused a significant interest on biofuels, especially ethanol and biodiesel. The combustion of liquid fuels in diesel engines, turbines, rocket engines and industrial furnaces depends on the effective atomization to increase the surface area of the fuel and thus to achieve high rates of mixing and evaporation. In order to promote combustion with maximum efficiency and minimum emissions, an injector must create a fuel spray that evaporates and disperses quickly to produce a homogeneous mixture of vaporized fuel and air. Blurry injectors can produce a spray of small droplets of similar sizes, provide excellent vaporization and mixing of fuel with air, low emissions of NO_x and CO, and high efficiency. This work describes the initial development of a blurry injector for biofuels. Theoretical droplet sizes are calculated in terms of feed pressures and mass flow rates of fuel and air. Droplet size distribution and average diameters are meassured by a laser system using a diffraction technique.*

Keywords*: Blurry injector, Liquid biofuels, Laser diffraction technique, Droplet size, Test bench*

1. INTRODUCTION

The continuous increase of oil prices and growing environmental concerns has raised interest in biofuels, especially ethanol and biodiesel. In addition, environmental legislation has become increasingly rigorous, setting rigid boundaries for the pollutants emissions of engines, turbines, furnaces, boilers and industrial combustion processes. Therefore, it is of interest to the country and companies to investigate the use of biofuels in industrial applications, aiming to reduce costs, increase operating efficiency and reduce pollutants emissions.

In general, before burning, liquid fuels are atomized through nozzles to form droplets, aiming to increase the contact area between the fuel and oxidizer and, therefore, to increase the rates of mixing and fuel evaporation. The reduction of droplet size leads to higher heat release rates per unit volume, facilitates the ignition of the mixture, extends the burning range and reduces the emissions of pollutants (Couto, 2007).

Many processes in the industry, in technological processes and medicine depend on the production of sprays with droplets of micrometric size. Various devices for liquid atomization have been developed, which can be called atomizers, nebulizers, injectors or nozzles. The atomization process occurs when a liquid jet, liquid sheet or a liquid film is disintegrated by the kinetic energy of the liquid itself, by exposure to a stream of air or gas of high speed, or as a result of external mechanical energy applied through rotating devices or vibrating (Lacava *et al.*, 2009). Due to the random nature of the atomization process, the resulting spray is usually characterized by a large spectrum of droplet size.

Based on a flow-focusing injector, Gañan-Calvo, 1998, developed the blurry type injector which presents several advantages over other injectors, such as formation of a uniform spray, better atomization, high atomization efficiency, robustness, excellent fuel vaporization and mixture with air, and potential for application in compact combustion systems which can be used as portable power sources. Panchasara *et al.* (2009) compared experimentally a blurry injector with a commercial air-blast injector, using kerosene and diesel burning in air at ambient pressure, and verified that the flow blurring injector produced 3 to 5 times lower NO_x and CO emissions as compared to the airblast injector. Sadasivuni and Agrawal (2009) used the blurry injector in a compact combustion system with a counter flow heat exchanger. The volumetric energy density of the system was substantially higher than that of the concepts developed previously. Heat release rate of up to 460 W was achieved in a combustor volume of 2.0 cm^3. The combustion system produced clean, compact, quiet, distributed, attached flat flame. No soot or coking problems were experienced during or after combustor operation on kerosene fuel.

Therefore, this work aims to present the initial development of a blurry injector for biofuels and to describe a bench for testing injectors. This injector will be later used in a flameless compact combustor. Flameless combustion is a homogeneous low temperature burning process leading to strongly reduced pollutant emissions and higher efficiency compared to traditional combustion processes (Wünning *et al.*, 1997).

2. OPERATIONAL PRINCIPLE OF A BLURRY INJECTOR

There are numerous ways of finely breaking up a liquid into droplets. The blurry injector uses a second fluid, normally a gas, to provide the energy necessary to finely divide and disperse the liquid into smaller fragments or particles.

The blurry injector yields a simple, reproducible, and robust flow pattern which gives rise to a gas-liquid interaction with a high efficiency. The flow geometry surpasses the efficiency of "prefilming air-blast atomizers," a highly efficient albeit complex and costly technological variety. This achievement is due to the unexpected emergence of a back-flow pattern leading to small-scale perturbations (Gañan-Calvo, 2005).

The flow-blurring injector consists of a nozzle for liquid injection and an orifice plate located downstream of the nozzle. Figure 1 shows a scheme of the blurry injector.

The liquid to be atomized exits from a feed tube whose inner diameter is equal to the exit orifice diameter *D*, as seen in Fig. 1. The outlet of the feed tube has the same diameter *D* as the exit orifice; both sections face each other, at an offset distance *H*. The end of the tube is sharp cut perpendicularly to its axis. Thus, the gap between the tube end and the exit orifice gives rise to a lateral cylindrical passageway, LCP. It is worth noting that the LCP surface equals the exit orifice area when $c = H/D = 0.25$. Consequently, when both a liquid mass flow rate $\dot{m}_l$ is forced through the tube and a gas mass flow rate $\dot{m}_g$ is forced through the LCP, a spray combining both phases is formed and leaves the device through the orifice exit.

The bifurcation separating the back-flow regime from a conventional flow-focusing pattern is triggered by a single fundamental geometrical parameter $c = H/D$. When *c* is decreased to about 0.25, a radical modification in the flow configuration is observed. There is the return of the gas flow into the feeding tube of the liquid, creating a recirculation flow within the tube, resulting in an intense mixture between the phases and thus creating an almost uniform spray of small droplets. When $c > 0.25$ the liquid flow follows a "flow focusing" pattern, with the formation of a liquid microjet (Gañan-Calvo, 2005).

Assuming a specific value of the liquid flow rate and the total energy input, the flow configuration creates about five to fifty times more surface than any other pneumatic atomizer of the "plain-jet airblast" type (Lefebvre, 1989).

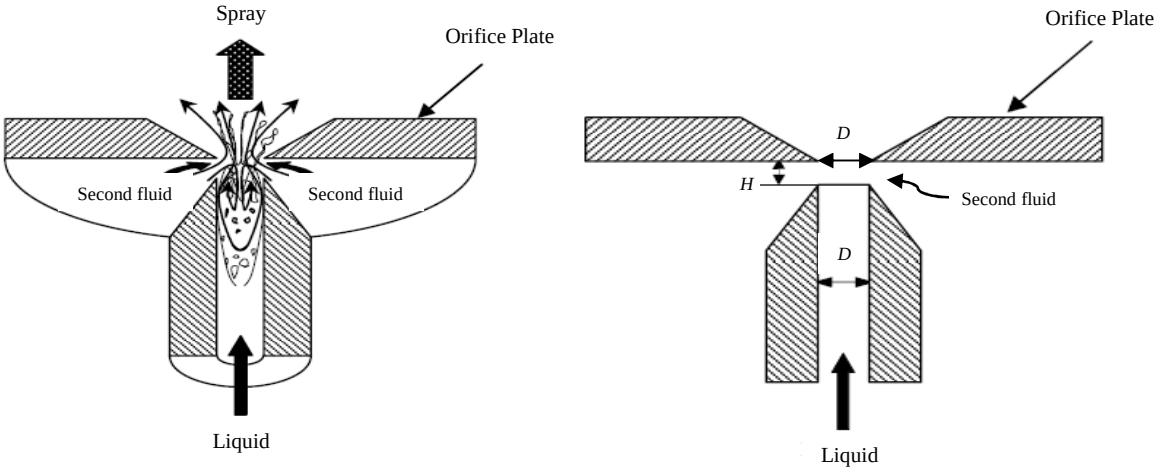

Figure 1. Schematic the Flow-Blurring Injector: flow structure and geometric details.
Reference Source: Adaptation, Panchasara, D. E., *et al*., 2009.

3. BLURRY INJECTOR AND TEST BENCH

3.1. Blurry Injector for Testing

A blurry injector with $D = 1$ mm was designed and built. The offset distance, *H*, is controlled by the action of a screw nut and can be varied from 0.15 mm to 0.30 mm.

Figure 2 shows a scheme and photos of a blurry injector and its components.

In order to minimize gas friction losses between the tube walls and the exit orifice walls when the ratio H/D is small, the tube end was sharpened with an angle of 60°.

Figure 3 shows a photo of a leaking test using water in the injector.

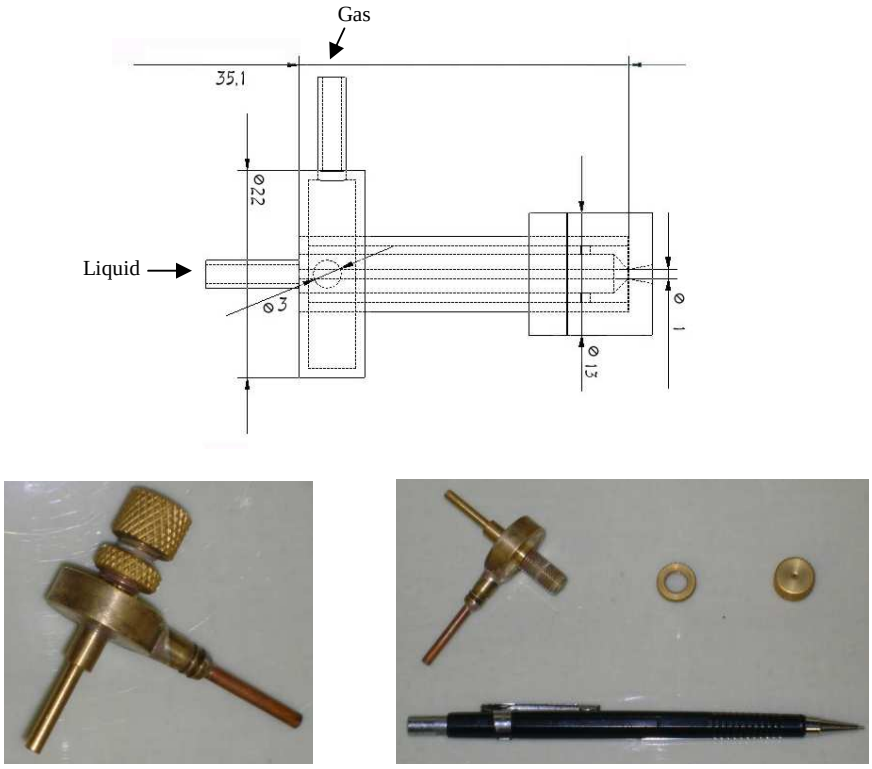

Figure 2. Schematic representation and photos of the Blurry injector.

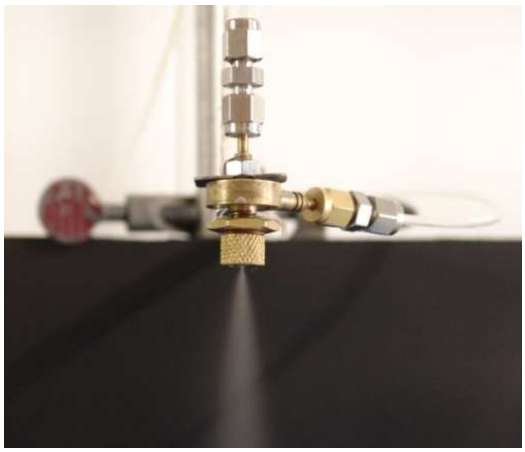

Figure 3. Photo of a leaking test of the blurry injector.

3.2. Test bench

A bench was designed and built for testing the blurry injector with biofuels. Figure 4 shows a scheme and photo of the test bench. The main components of the test bench are:

- Two tanks with 4 liters capacity each for storage of liquids to be atomized.
- One cylinder of nitrogen to pressurize the tanks. The reservoir may have its pressure adjusted by a valve.
- One cylinder of compressed air for atomization of the fuels.
- Two filters.
- Valves for pressure relief in the tanks, safety, filling and drainage of tanks and pressure control in the line.
- Two pressure regulators.
- Three pressure meters.
- ¼” piping.
- Malvern (Spraytec®) laser system for droplet size measurement.

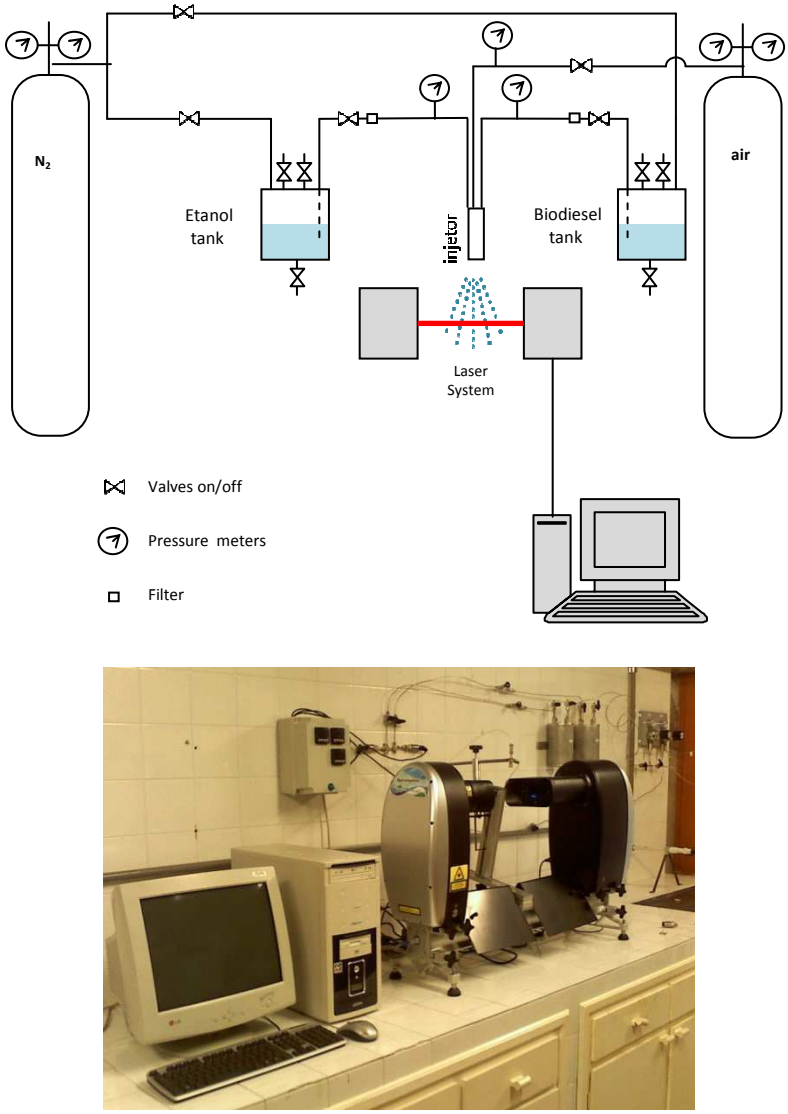

Figure 4. Schematic representation and photos of the test bench.

The pressure operational range of the bench is 0-8 bar and the following parameters can be measured:

- Discharge coefficient;
- Spray cone angle;
- Mean droplet sizes;
- Droplet size distribution;
- Mass flow distribution.

The laser system Spraytec® measures the size distributions of drops by a laser diffraction technique, without interfering in the liquid atomized. A laser beam passes through the spray, initially parallel, and then is diffracted by the droplets. Photodiodes located on a circular plate collect the scattered light. The system uses the Mie theory for analysis of the droplet size distribution. Mie Theory provides a rigorous solution for the calculation of particle size distributions from light scattering data and is based on Maxwell's electromagnetic field equations. This theory predicts the primary scattering response observed from the surface of the particle, with the intensity predicted by the refractive index difference between the particle and the dispersion medium. Size distributions of particles can be accurately measured by the Spraytec® system up to 98% obscuration, beyond the operating range of traditional laser diffraction systems. Obscuration is the percentage of the laser beam power which is not detected by the sensors (Dodge, 1984). The equipment is connected to a computer for data acquisition and treatment and a statistical software is used to analyze the data. Figure 5 shows a photo of the laser beam passing through the spray. The laser beam is not well seen in Fig. 5 due to the presence of a polycarbonate protection in front of the spray.

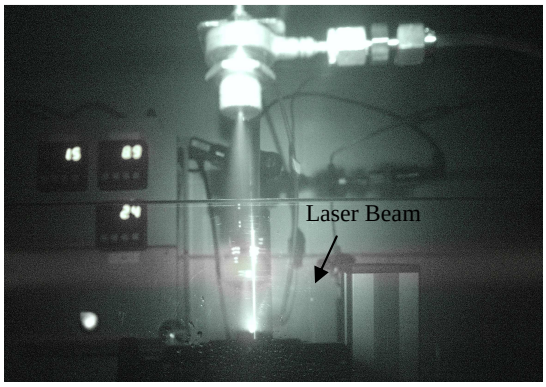

Figure 5. Photo of the laser beam crossing the spray.

4. THEORETICAL ANALYSIS

The mass flow rate of air in a blurry injector is calculated assuming sonic conditions at the orifice exit, and it is given by the following equation (Anderson, 2003):

$$\dot{m}_g = \frac{P_{0,g} A}{\sqrt{R T_{0,g}}} \left[\gamma \left(\frac{2}{\gamma+1} \right)^{\frac{\gamma+1}{\gamma-1}} \right]^{1/2} \tag{1}$$

where A is the area of exit orifice, γ the specific heat ratio, R the constant of the gas, and $P_{0,g}$ and $T_{0,g}$ are the gas reservoir pressure and temperature, respectively.

The pressure, temperature and density of gas at the orifice exit can be calculated, respectively, by:

$$P_g = P_{0,g} \left(\frac{2}{\gamma+1} \right)^{\frac{\gamma}{\gamma-1}} \tag{2}$$

$$T_g = T_{0,g} \frac{2}{\gamma+1} \tag{3}$$

$$\rho_g = \rho_{0,g} \left(\frac{2}{\gamma+1} \right)^{\frac{1}{\gamma-1}} \tag{4}$$

Considering an orifice diameter D = 1 mm, tank temperature $T_{0,g}$ = 298K, tank pressure $P_{0,g}$ = 3 bar, then $\dot{m}_g = 5.5\times10^{-4}$ kg/s, ρ_g = 2.223 kg/m^3 and v_g = 315.18 m/s.

Due the random nature of atomization process, involving dispersed populations of drops, the spray is usually characterized by droplet size distributions. The distributions correlate the volumetric percentage of a range of size drop in total volume of the drops population. To characterize a given drop size distribution are used representative mean diameters (Lefebvre, 1989).

The mass median diameter (MMD) corresponds to a drop diameter that encompasses 50% of the total mass or volume of a spray. Gañan-Calvo, 2005, obtained the following equation for the dimensionless mass median diameter (MMD/D) in a blurry injector with H/D = 0.25:

$$d = C_1 We^{-0.6} \left(1 + C_2 Oh\right) \left(1 + C_3 GLR^{-1}\right)^{1.2} \tag{5}$$

where d = MMD/D, C_1 = 0.42, C_2 = 18, C_3 =1, $GLR = \dot{m}_g / \dot{m}_l$ is the gas-to-liquid mass ratio, We is the Weber number and Oh is the Ohnesorge number.

The Weber number (We) is a measure of the relative importance between the inertia of the gas and liquid-gas surface tension and is given by:

$$We = \rho_g v_g^2 D \left(2\sigma\right)^{-1} \tag{6}$$

where ρ_g is the density of gas, v_g the gas velocity, both at the exit orifice, D is the diameter of the exit orifice and σ is the surface tension liquid-gas.

The Ohnesorge Number, *Oh*, is defined by the ratio of a viscous time (t_v) and a break-up time (t_b) and it is given by:

$$Oh = \mu_l \left(\rho_l \sigma D\right)^{-1/2} \tag{7}$$

The mass median diameter of the designed injector was calculated for several conditions, using water in the initial tests. Since it was adopted D = 1 mm, then d = MMD.

Considering ρ_l = 1000 kg/m^3, μ = 1.1 cPoise and σ = 73 mN/m, at T_o = 25 ^{o}C, ρ_g = 2.223 kg/m^3 and v_g = 315.18 m/s, it follows that *We* = 1512 and *Oh* = 0.004.

The kinetic energies per unit volume of liquid and gas are of the same order (Gañan-Calvo, 1998), then:

$$v_l \approx \left(\frac{\rho_g}{\rho_l}\right)^{\frac{1}{2}} v_g = 14.88 \text{ m/s} \tag{8}$$

Since v_l, A and ρ_l are known, then $\dot{m}_l = 1.2\times10^{-2}$ kg/s, therefore *GLR* = 0.0474 and *MMD* = 26.2 μm.

The same procedure is repeated for the gas reservoir pressure, $P_{0,g}$, varying from 3 to 8 bar, for $T_{0,g}$ = 298 K. The results are shown on Tab. 1.

Table 1. Theoretical droplet size as function of gas pressure.

P_{0g} [bar]	P_g [bar]	$\dot{m}_g$ [kg/s]	ρ_0 [kg/m^3]	ρ_g [kg/m^3]	v_g [m/s]	v_l [m/s]	$\dot{m}_l$ [kg/s]	*GLR*	*We*	*MMD* [μm]
3	1.584	0.00055	3.506	2.223	315.18	14.88	0.012	0.0474	1512	26.2
4	2.112	0.00074	4.675	2.964	318.04	17.34	0.014	0.0542	2053	20.4
5	2.64	0.00092	5.843	3.705	316.32	19.28	0.015	0.0610	2538	17.0
6	3.168	0.00110	7.012	4.446	315.18	21.05	0.016	0.0670	3024	14.7
7	3.696	0.00129	8.181	5.186	316.87	22.85	0.018	0.0720	3566	12.8
8	4.224	0.00147	9.349	5.927	315.95	24.36	0.019	0.0772	4052	11.5

As expected, an increase in gas pressure causes a decrease in the MMD droplet diameter, as well as causes an increase in the mass flow rates and velocities of gas and liquid.

5. SPRAY CHARACTERIZATION

The characterization of the blurry injector involves the determination of discharge coefficient, mean droplet sizes and spray cone angle as a function of the liquid and air tank pressures. Water was used in the initial tests.

5.1 Discharge coefficient

The discharge coefficient is used to correlate the liquid mass flow rate with the liquid pressure drop along the injector. In this case there is no air flow during the measurement.

Considering incompressible flow, adiabatic flow, no variation of gravitational potential energy, the discharge coefficient is obtained from the continuity equation (Delmeé, 1983):

$$c_d = \frac{\dot{m}_l}{A\sqrt{2\rho_l \Delta P_l}} \tag{9}$$

where $\Delta P_l = P_{l,inj} - P_{amb}$ is the drop pressure, P_{amb} is the ambient pressure and $P_{l,inj}$ is the liquid injection pressure. The liquid injection pressure is measured just before the injector and its value is about 0.1 to 0.2 bar lower than the liquid tank pressure. It is expected that the discharge coefficient does not change with liquid mass flow rate, in order to the liquid mass flow rate to vary only with $\Delta P_l^{1/2}$.

To determine the discharge coefficient, the liquid is collected in a graduated recipient during 50 s and after the liquid mass in the recipient is measured and the average mass flow rate in this period is calculated.

5.2 Mean droplet size

A commonly used representative diameter in a reactive spray is the Sauter mean diameter, SMD. It is denoted by D_{32} and is defined by:

$$D_{32} = \frac{\sum_{i=1}^{n} d_i^3}{\sum_{i=1}^{n} d_i^2} \tag{10}$$

Other representative diameters are the mass diameters D_{10}, D_{50} and D_{90}. These diameters correspond, respectively, to drop diameters that encompass 10%, 50% and 90% of total volume (or mass) of drops below the drop volume (or mass) considered. It should be noted that D_{50} is another notation for MMD.

5.3 Spray cone angle

Generally, the spray formed in the process of atomization has initially the shape of a cone. The opening angle is related to the penetration capability of the spray in the environment or combustion chamber (Lefebvre, 1989).

The spray cone angle is measured from digital photographs for each pre-defined condition. The photos are inserted into a treatment program image where two straight lines are drawn at the exit orifice tangent to the spray, allowing to measure the angle of the spray.

5.4 Experimental results

5.4.1 Discharge coefficient

Figure 6 shows the values of discharge coefficient obtained for the blurry injector with the liquid injection pressure ranging from 0.6 to 7 bar. Tests were conducted using the geometric parameter $c = H/D$ equal to 0.20 and 0.25. For the pressure range examined, the discharge coefficient was approximately constant, with average value 0.407 for H/D = 0.20 and 0.402 for H/D = 0.25.

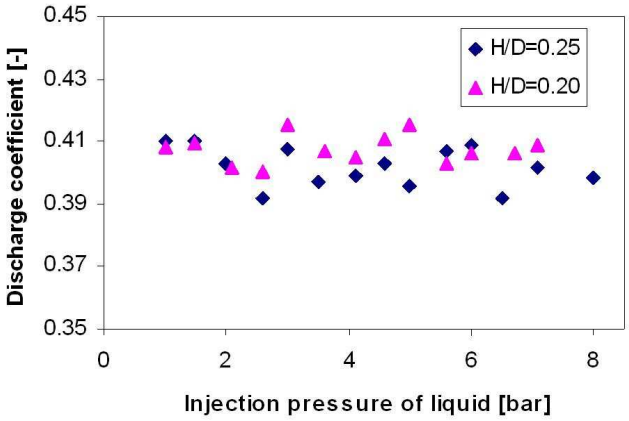

Figure 6. Discharge coefficient of the blurry injector without gas flow.

It is observed that regardless of the configuration H/D adopted the experimental values obtained for the coefficient of discharge are close. It is verified that the blurry regime also occurs for H/D = 0.20.

5.4.2 Spray cone angle

The spray cone angles for some operating conditions are presented in Figs. 7 and 8. In these figures $\Delta P_g = P_{g,inj} - P_{amb}$ where $P_{g,inj}$ is the injection pressure of air.

It is verified, in Figs. 7 and 8, an increase of spray angle for H/D = 0.25 compared to H/D = 0.2, for ΔP_l = 0.8 bar and $\Delta P_g = 1$ bar. However, it is not verified a change of spray angle for H/D = 0.25 compared to H/D = 0.2, for ΔP_l = 1.7 bar and $\Delta P_g = 2$ bar.

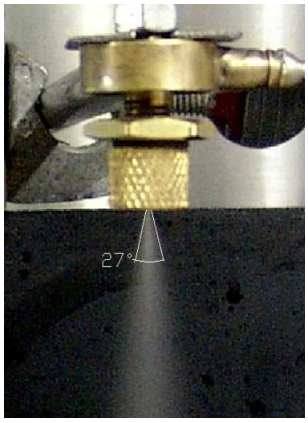

a) $\Delta P_l =$ 0.8 bar and $\Delta P_g = 1$ bar.

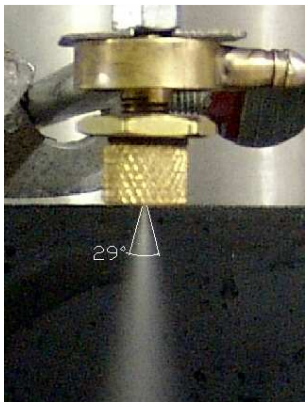

b) $\Delta P_l =$ 1.7 bar and $\Delta P_g = 2$ bar.

Figure 7. Spray cone angle with H/D = 0.20.

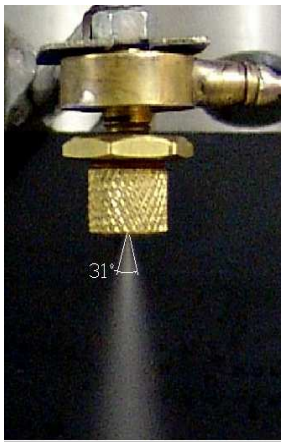

a) $\Delta P_l =$ 0.8 bar and $\Delta P_g = 1$ bar.

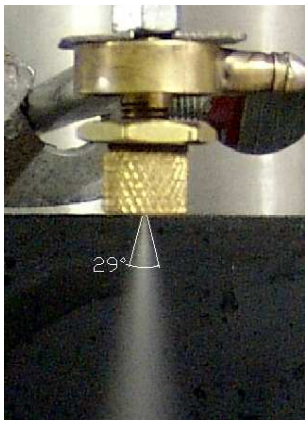

b) $\Delta P_l =$ 1.7 bar and $\Delta P_g = 2$ bar.

Figure 8. Spray cone angle with H/D=0.25.

5.4.3 Mean droplet size

Figure 9 shows plots of the droplet size distribution function (blue areas) and of the cumulative volume distribution function of droplet sizes (red line), as well as a table of the droplet size distribution function and of the cumulative volume distribution function of droplet sizes, for H/D = 0.2, with $P_{l,inj}$ = 1.5 bar and $P_{g,inj}$ = 2 bar.

Size (µm)	% V <	% V	Size (µm)	% V <	% V	Size (µm)	% V <	% V
0.117	0.00	0.00	2.51	9.08	1.67	54.12	98.66	0.93
0.136	0.00	0.00	2.93	10.95	1.86	63.10	99.14	0.47
0.158	0.00	0.00	3.41	13.06	2.11	73.56	99.35	0.21
0.185	0.00	0.00	3.98	15.51	2.45	85.77	99.44	0.10
0.215	0.00	0.00	4.64	18.42	2.91	100.00	99.52	0.07
0.251	0.00	0.00	5.41	21.91	3.49	116.59	99.61	0.09
0.293	0.00	0.00	6.31	26.11	4.20	135.94	99.73	0.12
0.341	0.00	0.00	7.36	31.10	4.99	158.49	99.85	0.12
0.398	0.00	0.00	8.58	36.92	5.81	184.79	99.95	0.10
0.464	0.00	0.00	10.00	43.49	6.57	215.44	100.00	0.05
0.541	0.01	0.01	11.66	50.65	7.17	251.19	100.00	0.00
0.631	0.15	0.14	13.59	58.17	7.51	292.87	100.00	0.00
0.736	0.45	0.30	15.85	65.72	7.55	341.46	100.00	0.00
0.858	0.91	0.47	18.48	72.97	7.25	398.11	100.00	0.00
1.00	1.56	0.65	21.54	79.61	6.63	464.16	100.00	0.00
1.17	2.39	0.83	25.12	85.35	5.74	541.17	100.00	0.00
1.36	3.40	1.01	29.29	90.03	4.68	630.96	100.00	0.00
1.58	4.57	1.18	34.15	93.60	3.57	735.64	100.00	0.00
1.85	5.92	1.34	39.81	96.11	2.51	857.70	100.00	0.00
2.15	7.42	1.50	46.42	97.73	1.62	1000.00	100.00	0.00

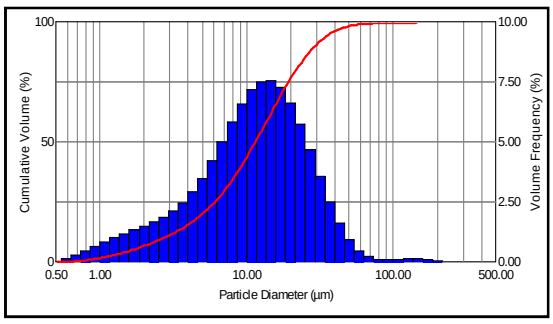

Figure 9. Experimental distribution of droplet diameters for a blurry injector with H/D = 0.2.

It is seen in the Table in Fig. 9 that only droplet diameters between 0.541 µm and 215.44 µm were detected by the laser Spraytec system. The Table in Fig. 9 indicates that D_{10}= 2.714 µm, D_{50} (MMD) =11.5 µm and D_{90}=29.26 µm. The Sauter Mean Diameter (D_{32}) was calculated by the system software as 6.214 µm.

Figure 10 shows the experimental results for the same fluid pressures of Fig. 9, however with *H*/*D*=0.25.

Size (µm)	% V <	% V	Size (µm)	% V <	% V	Size (µm)	% V <	% V
0.117	0.00	0.00	2.51	5.10	0.73	54.12	99.66	1.04
0.136	0.00	0.00	2.93	5.82	0.72	63.10	100.00	0.34
0.158	0.00	0.00	3.41	6.59	0.77	73.56	100.00	0.00
0.185	0.00	0.00	3.98	7.54	0.95	85.77	100.00	0.00
0.215	0.00	0.00	4.64	8.85	1.30	100.00	100.00	0.00
0.251	0.00	0.00	5.41	10.73	1.88	116.59	100.00	0.00
0.293	0.00	0.00	6.31	13.45	2.72	135.94	100.00	0.00
0.341	0.00	0.00	7.36	17.25	3.80	158.49	100.00	0.00
0.398	0.00	0.00	8.58	22.33	5.08	184.79	100.00	0.00
0.464	0.00	0.00	10.00	28.77	6.44	215.44	100.00	0.00
0.541	0.00	0.00	11.66	36.49	7.72	251.19	100.00	0.00
0.631	0.00	0.00	13.59	45.26	8.77	292.87	100.00	0.00
0.736	0.11	0.11	15.85	54.67	9.41	341.46	100.00	0.00
0.858	0.38	0.27	18.48	64.19	9.52	398.11	100.00	0.00
1.00	0.82	0.44	21.54	73.25	9.06	464.16	100.00	0.00
1.17	1.40	0.58	25.12	81.31	8.06	541.17	100.00	0.00
1.36	2.09	0.69	29.29	87.97	6.66	630.96	100.00	0.00
1.58	2.84	0.76	34.15	93.03	5.06	735.64	100.00	0.00
1.85	3.62	0.78	39.81	96.51	3.48	857.70	100.00	0.00
2.15	4.38	0.76	46.42	98.61	2.10	1000.00	100.00	0.00

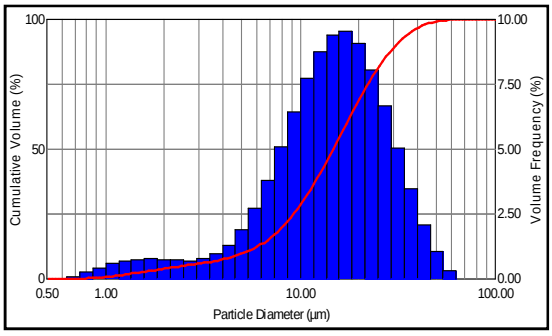

Figure 10. Experimental distribution of droplet diameters for a blurry injector with *H*/*D* = 0.25.

It is seen in the Table in Fig. 10 that only droplet diameters between 0.736 µm and 63.10 µm were detected. The Table in Fig. 10 indicates that D_{10}= 4.949 µm, D_{50} (MMD) =14.37 µm and D_{90}=31.36 µm. The Sauter Mean Diameter (D_{32}) calculated by the system software is 8.448 µm.

The experimental Sauter mean diameters and mass median diameters are presented in Figs. 11 and 12 for different injection pressures with the configurations *H*/*D* = 0.20 and *H*/*D* = 0.25.

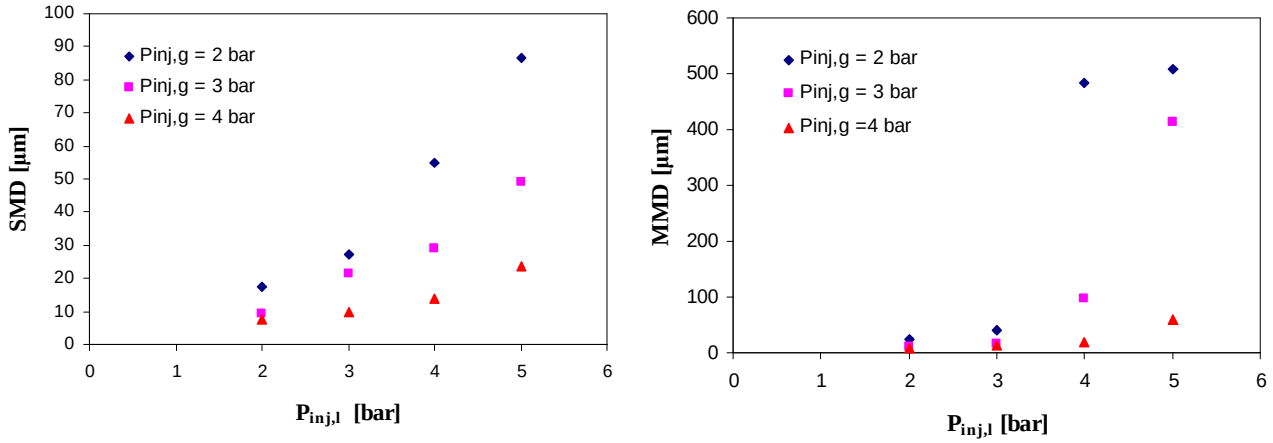

Figure 11. Experimental Sauter mean diameter (SMD) and mass median diameter (MMD) for *H*/*D* = 0.20.

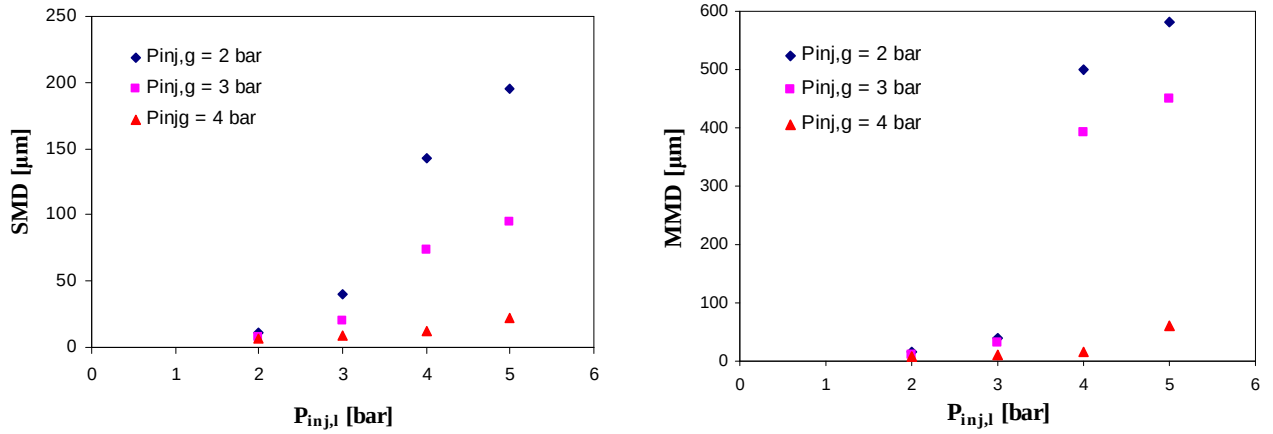

Figure 12. Experimental Sauter mean diameter (SMD) and mass median diameter (MMD) for *H*/*D* = 0.25.

As expected, it is observed that an increase in the injection pressure of liquid leads to an increase in SMD and MMD, and an increase in the injection pressure of air causes a decrease in SMD and MMD for both configurations. For injection pressure of air 2 and 3 bar it is observed an abrupt increase of the droplet size. For injection pressures of

liquid above the injection pressure of air, air cannot flow into the liquid tube and does not mixes turbulently with the incoming liquid, there is no blurring effect, but the generation of a microjet.

It is verified that SMD and MMD are smaller for $H/D = 0.20$ for low pressure, but close to the obtained values for $H/D = 0.25$ at higher injection pressures of air.

Table 2 shows the experimental and theoretical mass median diameters and experimental Sauter mean diameters with different injection pressures, for $H/D = 0.25$.

Table 2. Experimental mass median diameter (MMD) and Sauter mean diameter (SMD) considering $H/D = 0.25$.

$P_{g,inj}$ [bar]	$P_{l,inj}$ [bar]	MMD [μm] experimental	MMD [μm] theoretical
2	3	32.07	36.7
3	3	26.85	26.2
4	3	17.33	20.4
5	3	15.96	17.0
6	3	13.88	14.7

Experimental results show a maximum error of about 15% with respect to the theoretical results. It is verified that an increase in the injection pressure of air causes a decrease in MMD.

6. CONCLUSIONS

This paper presented the initial development of a blurry injector for burning biofuels. A bench was designed and prepared for testing the injector. Theoretical droplet diameters were calculated and compared to the experimental data. Discharge coefficients, spray angles, distribution of droplet sizes and average diameters were determined experimentally.

7. ACKNOWLEDGEMENTS

The authors acknowledge Vale Energy Solutions for providing a scholarship to the first author.

8. REFERENCES

Anderson, J. D. 2003, “Modern Compressible Flow: With Historical Perspective”, New York: McGraw-Hill Science/Engineering/Math, 3 edition, 650 p.

Couto, H.S., 2007, “Atomização e Sprays”, Apostila I Escola de Combustão, Florianópolis, Santa Catarina, Brazil.

Delmeé G. J,. 1983, “Manual de Medição de Vazão”, São Paulo: Editora Edgard Blucher. 474p.

Dodge, L.G., 1984, “Change of calibration of diffraction based particle sizes in dense sprays”, Optical Engineering, Vol. 23, Nº5, p. 626-630.

Gañán-Calvo, A. M., 1998, “Generation of Steady Liquid Microthreads and Micro-Sized Monodisperse Sprays in Gas Streams”, Physical Review Letters, Vol.80, Nº2, p. 285-288.

Gañán-Calvo, A. M., Barrero, A. 1999, “A Novel Pneumatic Technique to Generate Steady Capillary Microjets”, J. Aerosol Sci., Vol.30, p. 117-125.

Gañán-Calvo, A. M., 2005, “Enhanced Liquid Atomization: From Flow-Focusing to Flow-Blurring”, Applied Physics Letters 86.

Lacava, P. T., Alves, A., 2009, “Capítulo 3: Injeção de Combustível”, Apostila II Escola de Combustão, p.68-111. São José dos Campos, São Paulo, Brazil.

Lefebvre, A.H., 1989, “Atomization and Sprays”, Taylor and Francis, New York.

Panchasara, H. V., Sequera, D. E., Schreiber, W. C., Agrawal, A. K., 2009, “Emissions Reductions in Diesel and Kerosene Flames Using a Novel Fuel Injector”, Journal of Propulsion and Power. Vol. 25, No. 4.

Sadasivuni, V., Agrawal, A. K., 2009, “A novel meso-scale Combustion System for Operation with Liquid Fuels”, Proceedings of the Combustion Institute, 32, p. 3155–3162.

Wünning, J. A., Wünning, J. G., 1997, **“**Flameless Oxidation to Reduce Thermal No-formation”, Progress in Energy and Combustion Science, 23, Issue 1, 1997, p.81-94.

6. RESPONSIBILITY NOTICE

The authors are the only responsible for the printed material included in this paper.